

Synthesis and electrochemical properties of $\text{LiNi}_{1-y}\text{Zn}_y\text{O}_2$

Bok-Hee Kim · Jong-Hwan Kim · Sang-Jae Han ·
Su-Jin Hong · Myoung-Youp Song

Received: 31 May 2007 / Accepted: 18 March 2008 / Published online: 12 April 2008
© Springer Science + Business Media, LLC 2008

Abstract Zn doped $\text{LiNi}_{1-y}\text{Zn}_y\text{O}_2$ ($0.00 \leq y \leq 0.100$) composition was synthesized by an emulsion method. The emulsion-derived powder was calcined at the temperature range of 650–800 °C for 12–48 h. A single phase of $\text{LiNi}_{1-y}\text{Zn}_y\text{O}_2$ was obtained at 700 °C. The optimum condition for the synthesis of $\text{LiNi}_{1-y}\text{Zn}_y\text{O}_2$ was to be calcined at 750 °C for 36 h in oxygen stream. The composition of $\text{LiNi}_{0.995}\text{Zn}_{0.005}\text{O}_2$ showed the largest discharge capacity and improved cycle life. The initial and final discharge capacities were 163 and 154.5 mAh/g, respectively. The fading rate in discharge capacity after 20 cycles was only 5.2%.

Keywords Powder synthesis · Discharge capacity · $\text{LiNi}_{1-y}\text{Zn}_y\text{O}_2$ · Cathode material · Emulsion method

1 Introduction

LiNiO_2 is well known as one of promising cathode materials for the Li-secondary battery because it has the high capacity, low cost and environmental pollution compared with LiCoO_2 [1, 2]. But it exhibits severe capacity fading due to transition from LiNiO_2 to $\text{Li}_{1-x}\text{Ni}_{1+x}\text{O}_2$ during the charge-discharge cycling. The deterioration of discharge capacity is from the crystal structural instability [3].

Several cations were added into LiNiO_2 and $\text{LiNi}_{0.8}\text{Co}_{0.2}\text{O}_2$ to replace Ni in order to stabilize the crystal structure and enhance the electrochemical properties [4, 5]. Al substitution suppresses the phase transition during cycling, improves the cycle life and reduces the capacity fading of the LiNiO_2 [6–8]. Substitution with Mg and Ti for Ni in LiNiO_2 and $\text{LiNi}_{0.8}\text{Co}_{0.2}\text{O}_2$ improved the capacity and safety characteristics [9, 10]. Recently we reported the effect of substituting Ni in LiNiO_2 with Al, which was found to improve the discharge capacity and the cycling stability [11].

Thus electro-inactive non-transition metal ions have been investigated extensively as the dopants to stabilize the crystal structure and improve the electrochemical properties of the cathode materials. However, one of the non-transition metal ions, Zn^{2+} has not attraction as substitute ion for Ni in LiNiO_2 cathode materials. In this research, crystal structure and electrochemical properties of Zn-doped LiNiO_2 were investigated upon the synthesis conditions.

2 Experimental procedure

$\text{LiOH} \cdot \text{H}_2\text{O}$ (99.95%, Aldrich Chemical Company, Inc.), Ni $(\text{NO}_3)_2 \cdot 6\text{H}_2\text{O}$ (99.99%, High Purity Chemicals, Japan), and $\text{Zn}(\text{NO}_3)_2 \cdot 6\text{H}_2\text{O}$ (99.9%, High Purity Chemicals, Japan) were chosen as starting materials and dissolved in distilled water. Precursor solution (0.5 mol/l for the $\text{LiNi}_{1-y}\text{Zn}_y\text{O}_2$ composition) was prepared by mixing of each aqueous solution on a magnetic stirrer for 24 h. The water-in-oil type emulsion of $\text{LiNi}_{1-y}\text{Zn}_y\text{O}_2$ composition was prepared using the precursor and organic phase according to the same process as already reported [12–14]. The emulsion was sprayed into the kerosene heated to 170 °C to

B.-H. Kim (✉) · J.-H. Kim · S.-J. Han · S.-J. Hong · M.-Y. Song
Division of Advanced Materials Engineering,
Hydrogen & Fuel Cell Research Center,
Chonbuk National University,
1-664-14, Duckjin-dong, Duckjin-ku,
Chonju City, Chonbuk 561-756, South Korea
e-mail: kimbh@chonbuk.ac.kr

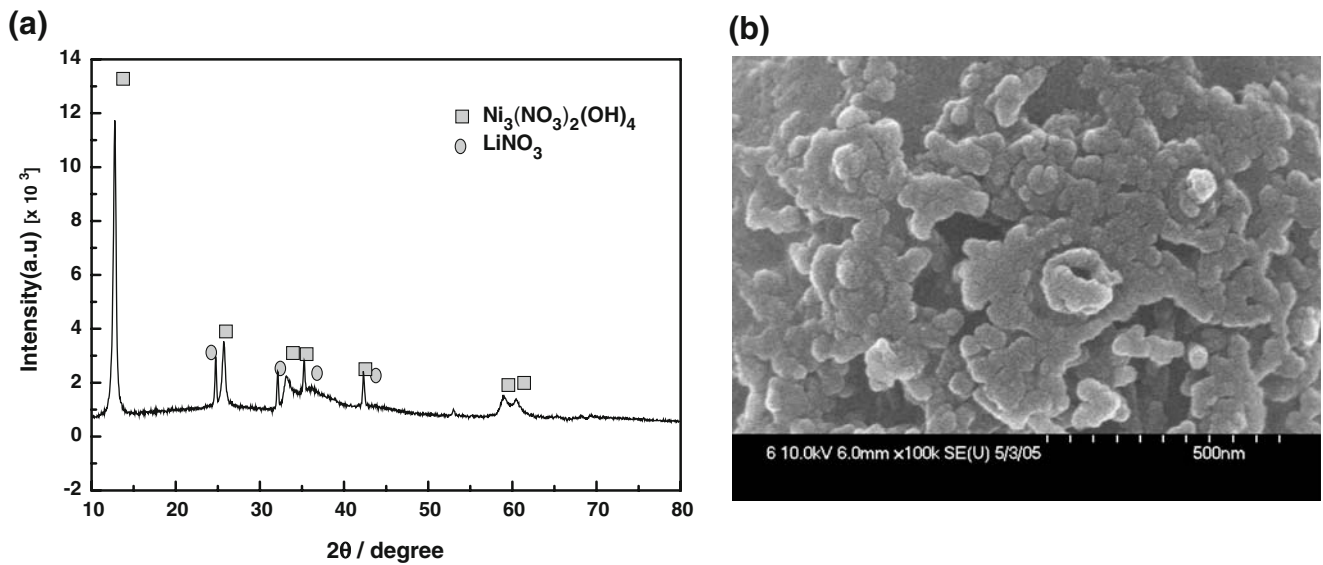


Fig. 1 XRD pattern (a) and SEM photograph (b) of as-dried powder

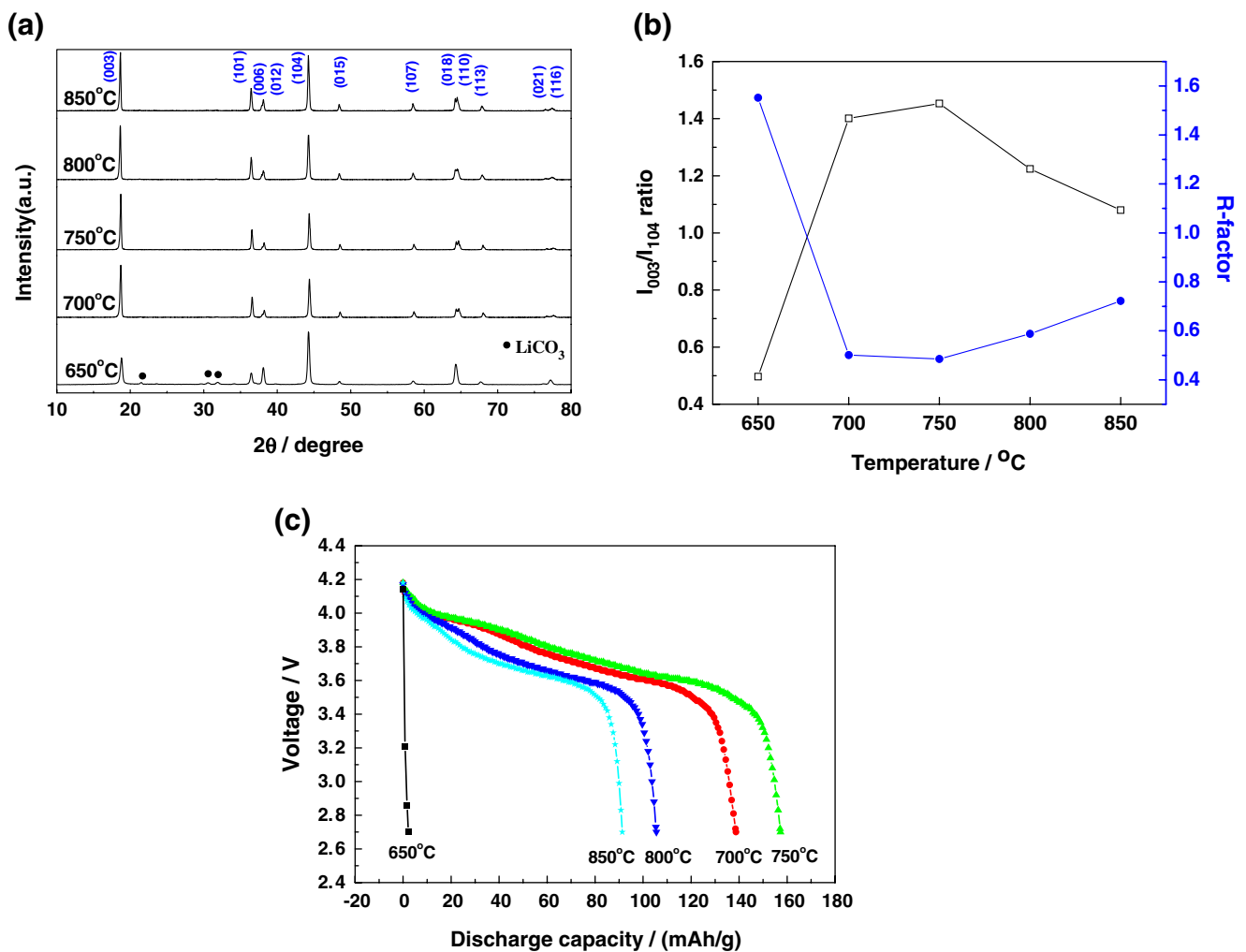


Fig. 2 XRD patterns (a), I_{003}/I_{104} ratios, R -factors (b) and discharge capacities (c) of $\text{LiNi}_{0.990}\text{Zn}_{0.010}\text{O}_2$ powder synthesized at 650~850 °C for 24 h

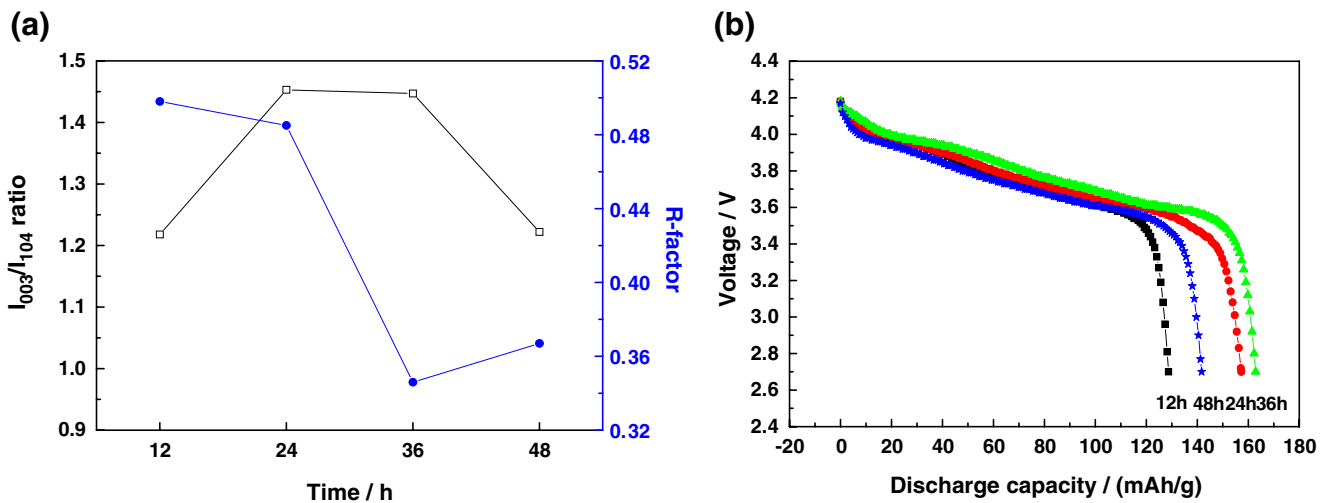


Fig. 3 I_{003}/I_{104} ratios, R -factors (a) and first discharge capacities (b) of $\text{LiNi}_{0.990}\text{Zn}_{0.010}\text{O}_2$ powder calcined at 750°C for various times

evaporate water included in emulsion and dried at 120°C in the oven. As-dried powders were calcined at the temperature of $650\text{--}850^\circ\text{C}$ for various times in an oxygen stream with heating and cooling rates of $1^\circ\text{C}/\text{min}$.

The calcined powders were examined by an X-ray diffractometer (XRD: Rigaku, D/MAX-111A) and scanning electron microscope (SEM: JEOL JSM-6400). The electrochemical properties were measured at room temperature with a half cell of Li metal/electrolyte 1M LiPF_6 -ethylene carbonate (EC) and dimethyl carbonate (DMC) (1:1 in volume)/cathode material. The positive materials consisted of $\text{LiNi}_{1-y}\text{Zn}_y\text{O}_2$ powder, acetylene black and PTFE at the ratio of 88:10:2 by weight. Lithium foil and glass micro-fibre filters (GF/A, Whatman) were used for the anode and separator, respectively. The cells were automatically charged and discharged in the range of between 2.7 and 4.2 V at 9.5 mA/g for 20 cycles.

3 Results and discussion

Among the $\text{LiNi}_{1-y}\text{Zn}_y\text{O}_2$ ($0.00 \leq y \leq 0.100$) compositions, $\text{LiNi}_{0.990}\text{Zn}_{0.010}\text{O}_2$, was selected to investigate the particle shape and optimum calcination temperature and time.

The XRD pattern and SEM photograph of the as-dried powder of $\text{LiNi}_{0.990}\text{Zn}_{0.010}\text{O}_2$ composition are shown in Fig. 1. The XRD pattern in Fig. 1(a) was identified as being composed of the crystal phases of LiNO_3 and $\text{Ni}_3(\text{NO}_3)_2(\text{OH})_4$. LiNO_3 and $\text{Ni}_3(\text{NO}_3)_2(\text{OH})_4$ phases formed during drying are different from the starting materials, but Zn compound is not shown in this figure. This means that these crystal phases were formed during drying by the reaction of various component ions such as Li^+ , Ni^{2+} and NO_3^- which were dissolved in the water. The SEM photograph in Fig. 1(b) shows the agglomerated shape with nanosized particles.

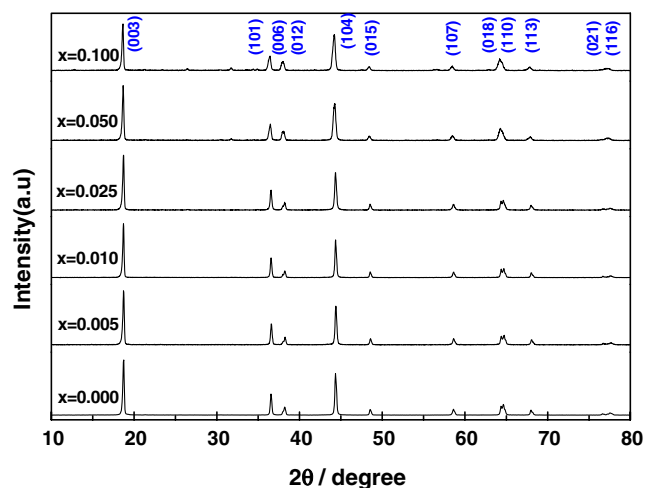


Fig. 4 XRD patterns of $\text{LiNi}_{1-y}\text{Zn}_y\text{O}_2$ powder synthesized at 750°C for 36 h

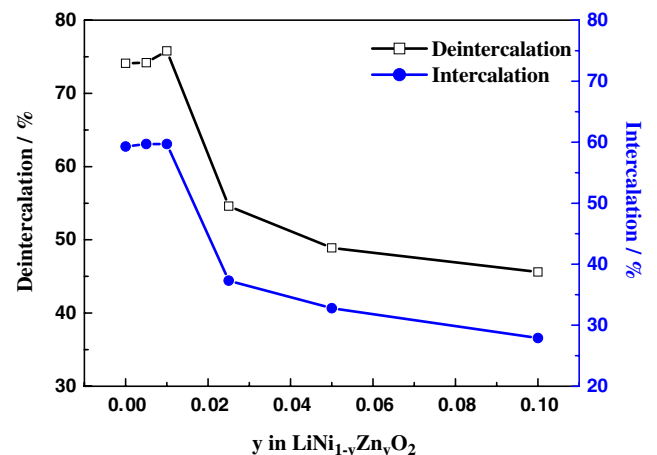


Fig. 5 The deintercalation and intercalation of Li^+ in $\text{LiNi}_{1-y}\text{Zn}_y\text{O}_2$

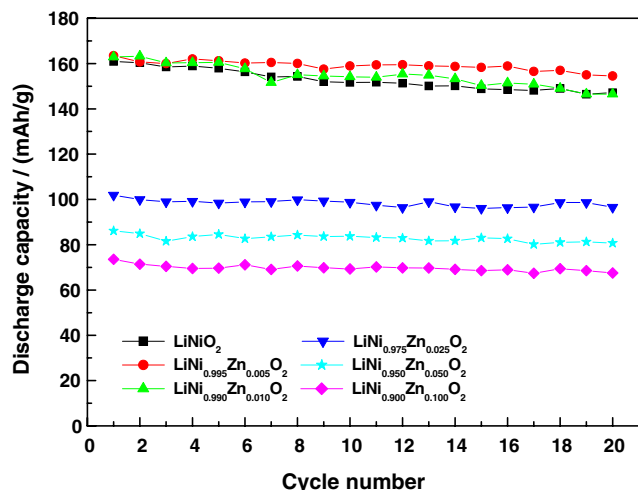


Fig. 6 Cyclic discharge capacities of $\text{LiNi}_{1-y}\text{Zn}_y\text{O}_2$

Figure 2 shows the XRD patterns, I_{003}/I_{104} ratios, R -factors and discharge capacities of the $\text{LiNi}_{0.990}\text{Zn}_{0.010}\text{O}_2$ powder synthesized at $650\sim 850\text{ }^\circ\text{C}$ for 24 h under oxygen gas stream. In Fig. 2(a), the crystal phase of the powder calcined at $650\text{ }^\circ\text{C}$ was mainly a layered structure with a little Li_2CO_3 . This compound was formed during calcination of emulsion-derived powder due to the reaction between Li^+ and organic phase and remained as an unreacted phase at $650\text{ }^\circ\text{C}$. All the powders calcined above $700\text{ }^\circ\text{C}$ exhibited a single phase of the layered structure. The analysis of these XRD patterns indicated that $\text{LiNi}_{0.990}\text{Zn}_{0.010}\text{O}_2$ single phase could be synthesized above $700\text{ }^\circ\text{C}$. In Fig. 2(b), I_{003}/I_{104} ratio increased to maximum value of 1.45 at $750\text{ }^\circ\text{C}$ and then decreased with elevated temperature, but R -factor decreased to minimum value of 0.49 at $750\text{ }^\circ\text{C}$ and increased with elevated temperature. The powder synthesized at $750\text{ }^\circ\text{C}$ shows the highest I_{003}/I_{104} value of 1.45 and the lowest R -factor of 0.49. This means that the powder with the lowest cation mixing [15] and the highest hexagonal ordering [16] could be expected to have good electrochemical properties. From Fig. 2(c) of first discharge capacities, the powder synthesized at $750\text{ }^\circ\text{C}$ has the highest value of 158.5 mAhg^{-1} at the initial discharge as expected above. This result shows that the optimum temperature to synthesize $\text{LiNi}_{0.990}\text{Zn}_{0.010}\text{O}_2$ powders is $750\text{ }^\circ\text{C}$.

All the crystal phase of $\text{LiNi}_{0.990}\text{Zn}_{0.010}\text{O}_2$ powders synthesized at $750\text{ }^\circ\text{C}$ for various times showed single layered structure. The I_{003}/I_{104} ratios, R -factors and discharge capacities are shown in Fig. 3. In Fig. 3(a), the I_{003}/I_{104} ratio increased to maximum value of 1.45 at $24\sim 36\text{ h}$ and then decreased with elevated temperature, but R -factor decreased to minimum value of 0.35 at 36 h and increased again with elevated temperature. The powder synthesized for 36 h has the highest I_{003}/I_{104} value of 1.45 and the lowest value of 0.35. This means that the powder has the lowest cation mixing and the highest hexagonal ordering and could be expected to have good electrochemical properties. From Fig. 3(b) of first discharge capacities, the powder synthesized at $750\text{ }^\circ\text{C}$ for 36 h has the highest value of 163 mAhg^{-1} .

From the above results, it was determined that the optimum condition to synthesize $\text{LiNi}_{0.99}\text{Al}_{0.01}\text{O}_2$ was heating at $750\text{ }^\circ\text{C}$ for 36 h. Therefore, the complete experimental range of compositions, $\text{LiNi}_{1-y}\text{Zn}_y\text{O}_2$ ($y=0.000, 0.005, 0.010, 0.025, 0.050, 0.100$), were synthesized at this condition. The XRD patterns of powders synthesized at this condition were shown in Fig. 4. All the XRD patterns show the single layered structure without any relation to the amount of Zn addition. The lattice parameter a and c obtained from XRD patterns increased with increasing the amount of Zn addition.

The deintercalation–intercalation of Li^+ was measured using $\text{Li}/\text{LiNi}_{1-y}\text{Zn}_y\text{O}_2$ cells operated between 2.7 and 4.2 V and shown in Fig. 5. In Fig. 5, the deintercalation and intercalation fraction of Li^+ was almost same with the value of 0.74–0.76 and 0.60 respectively in the compositions of $y=0.000\sim 0.010$, but was decreased largely above $y=0.025$ in $\text{LiNi}_{1-y}\text{Zn}_y\text{O}_2$. This means that substitution of Ni with Zn until 0.010 fraction almost has no effect on the deintercalation–intercalation of Li^+ but Zn above 0.025 fraction affected largely. It could be expected that $\text{LiNi}_{1-y}\text{Zn}_y\text{O}_2$ was more stable than LiNiO_2 structure due to the fixed atomic valance of Zn^{2+} instead of unstable Ni ion and stable structure enabled Li^+ to intercalate easily. The good cycle life of charge–discharge property also was considered from easy intercalation reaction [17]. However, excess over some amount of Zn substitution also would make Li^+ difficult to intercalate into the structure because of the fixed valance of the zinc ion.

Table 1 The discharge capacities and fading rates of $\text{LiNi}_{1-y}\text{Zn}_y\text{O}_2$.

Parameter	Value					
y in $\text{LiNi}_{1-y}\text{Zn}_y\text{O}_2$	0.000	0.005	0.010	0.025	0.050	0.100
1st discharge capacity (mAh/g)	160.9	163.0	162.9	102.0	86.1	73.6
Final discharge capacity after 20 cycles (mAh/g)	147.1	154.5	146.5	96.5	80.7	67.5
Fading rate (%)	8.6	5.2	10.1	5.4	5.4	6.1

The cyclic charge-discharge properties of $\text{LiNi}_{1-y}\text{Zn}_y\text{O}_2$ powder calcined at 750 °C for 36 h were measured for 20 cycles and are shown in Fig. 6. The first discharge capacity and fading rate according to the cycles of charge-discharge test are listed in Table 1. Most of these compositions show the improvement of fading rate except $\text{LiNi}_{0.990}\text{Zn}_{0.010}\text{O}_2$. This composition shows the higher first discharge capacity and almost same with LiNiO_2 after 20 cycles, but the fading rate is lower than any other composition because of the higher discharge capacity. The composition of $\text{LiNi}_{0.995}\text{Zn}_{0.005}\text{O}_2$ powder shows the highest discharge capacity, 163 mAh/g and the lowest fading rate 5.2%. The electrochemical property was improved by substituting 0.005 fraction of Ni ion with Zn ion in LiNiO_2 as expected above.

As discussed above, the substitution of nickel ion with zinc ion in LiNiO_2 increases the crystal structure stability but also makes Li^+ difficult to intercalate into the crystal structure because of the fixed valance of zinc ion. This decreases the discharge capacity of the $\text{LiNi}_{1-y}\text{Zn}_y\text{O}_2$, but improved fading rate by the structural stability. However, $\text{LiNi}_{0.995}\text{Zn}_{0.005}\text{O}_2$ shows the highest discharge capacity and lowest fading rate. These results suggest that substituting Ni with an optimum amount of Zn^{2+} in LiNiO_2 raises the crystal structure stability, increases the discharge capacity and lowers the fading rate of discharge capacity due to the fixed atomic valence of Zn.

4 Conclusion

The cathode material, $\text{LiNi}_{1-y}\text{Zn}_y\text{O}_2$, was synthesized by emulsion method and calcined at various temperatures and times in an oxygen stream. The most suitable calcination condition was determined to be heating at 750 °C for 36 h. The discharge capacity of $\text{LiNi}_{1-y}\text{Zn}_y\text{O}_2$ increased a little until $y=0.010$ and decreased above $y=0.025$. However, $\text{LiNi}_{0.995}\text{Zn}_{0.005}\text{O}_2$ showed the highest discharge capacity and improved cycle life. The initial and final discharge capacities after 20 cycles were 163 and 154.5 mAh/g,

respectively. The fading rate of discharge capacity was only 5.2% after 20 cycles of charge-discharge.

Acknowledgement This work was supported by grant No. R01-2003-000-10325-0 from the Basic Research Program of the Korea Science & Engineering Foundation.

References

1. T. Ohzuku, A. Ueda, *Solid State Ion.* **69**, 201 (1994). DOI [10.1016/0167-2738\(94\)90410-3](https://doi.org/10.1016/0167-2738(94)90410-3)
2. M. Broussely, F. Pertion, P. Biensan, J.M. Bodet, J. Labat, A. Lecerf, C. Delmas, A. Rougier, J.P. Peres, *J. Power Sources* **54**, 109 (1995). DOI [10.1016/0378-7753\(94\)02049-9](https://doi.org/10.1016/0378-7753(94)02049-9)
3. C.C. Chang, P.N. Kumta, *J. Power Sources* **75**, 44 (1998). DOI [10.1016/S0378-7753\(98\)00091-3](https://doi.org/10.1016/S0378-7753(98)00091-3)
4. S.H. Chang, S.G. Kang, S.W. Song, J.B. Yoon, J.H. Choy, *Solid State Ion.* **86–88**, 171 (1996). DOI [10.1016/0167-2738\(96\)00117-8](https://doi.org/10.1016/0167-2738(96)00117-8)
5. Y. Gao, M.V. Yakovleva, W.B. Ebner, *Electrochem. Solid-State Lett.* **1**(3), 117 (1998). DOI [10.1149/1.1390656](https://doi.org/10.1149/1.1390656)
6. T. Ohzuku, A. Ueda, M. Koguchi, *J. Electrochem. Soc.* **142**(12), 4033 (1995). DOI [10.1149/1.2048458](https://doi.org/10.1149/1.2048458)
7. T. Ohzuku, T. Yanagawa, M. Koguchi, A. Ueda, *J. Power Sources* **68**(1), 131 (1997). DOI [10.1016/S0378-7753\(97\)02516-0](https://doi.org/10.1016/S0378-7753(97)02516-0)
8. S.H. Park, K.S. Park, Y.K. Sun, K.S. Nahm, Y.S. Lee, M. Yoshio, *Electrochem. Acta* **46**, 1215 (2001). DOI [10.1016/S0013-4686\(00\)00710-6](https://doi.org/10.1016/S0013-4686(00)00710-6)
9. Y. Gao, M. Yakovleva, E. Ebner, A. Quinn, R. Schwindeman, B. Fitch, *J. Engel* (Electrochemical Society, Fall Meeting, Boston, USA, 1998)
10. V. Subramanian, G.T.K. Fey, *Solid State Ion.* **148**, 351 (2002). DOI [10.1016/S0167-2738\(02\)00073-5](https://doi.org/10.1016/S0167-2738(02)00073-5)
11. B.-H. Kim, J.-H. Kim, S.-J. Han, S.-J. Hong, M.-Y. Song, *J. Ceram. Soc. Jpn.* **115**(4), 245 (2007). DOI [10.2109/jcersj.115.245](https://doi.org/10.2109/jcersj.115.245)
12. B.-H. Kim, J.-W. Moon, J.-Y. Lee, Y.-K. Choi, *J. Ceram. Soc. Jpn.* **107**(1242), 115 (1999)
13. Y.-K. Choi, B.-H. Kim, *J. Ceram. Soc. Jpn.* **108**(1255), 261 (2000)
14. B.-H. Kim, Y.-K. Choi, Y.-H. Choa, *Solid State Ion.* **158**, 281 (2003). DOI [10.1016/S0167-2738\(02\)00909-8](https://doi.org/10.1016/S0167-2738(02)00909-8)
15. T. Ohjuku, A. Ueda, M. Nagayama, *J. Electrochem. Soc.* **140**, 1862 (1993). DOI [10.1149/1.2220730](https://doi.org/10.1149/1.2220730)
16. J.N. Reimers, E. Rossen, C.D. Jones, J.R. Dahn, *Solid State Ion.* **61**, 335 (1993). DOI [10.1016/0167-2738\(93\)90401-N](https://doi.org/10.1016/0167-2738(93)90401-N)
17. B.-H. Kim, J.-H. Kim, S.-J. Han, S.-J. Hong, M.-Y. Song, *J. Ceram. Soc. Jpn.* **115**(4), 245 (2007). DOI [10.2109/jcersj.115.245](https://doi.org/10.2109/jcersj.115.245)